

## Three-dimensional grids based on graphene oxide and 3,3',4,4'-tetraaminodiphenyl oxide for supercapacitor electrodes

Elena N. Gorenskaia,<sup>\*a</sup> Bato Ch. Kholkhoev,<sup>a</sup> Boris D. Ochirov,<sup>a</sup> Viktor G. Makotchenko,<sup>b</sup> Stepan I. Yusin,<sup>c</sup> Vladimir E. Fedorov<sup>b</sup> and Vitaliy F. Burdukovskii<sup>a</sup>

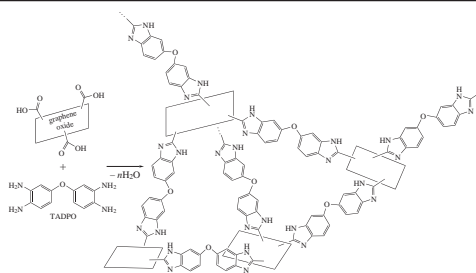
<sup>a</sup> Baikal Institute of Nature Management, Siberian Branch of the Russian Academy of Sciences, 670047 Ulan-Ude, Russian Federation. E-mail: gorenskaia.elena@mail.ru

<sup>b</sup> A. V. Nikolaev Institute of Inorganic Chemistry, Siberian Branch of the Russian Academy of Sciences, 630090 Novosibirsk, Russian Federation. E-mail: fed@niic.nsc.ru

<sup>c</sup> Institute of Solid State Chemistry and Mechanochemistry, Siberian Branch of the Russian Academy of Sciences, 630128 Novosibirsk, Russian Federation. E-mail: yusin.s@ya.ru

DOI: 10.1016/j.mencom.2018.03.025

New three-dimensional grids based on graphene oxide and 3,3',4,4'-tetraaminodiphenyl oxide were obtained using a one-step hydrothermal synthesis. The formation of benzimidazole rings was confirmed by IR spectroscopy and elemental analysis, and the nitrogen content was 13.8 wt%. Because of the redox activity of benzimidazole rings, the specific capacitance was 330 F g<sup>-1</sup> at a scan rate of 2 mV s<sup>-1</sup>.



Rising levels of energy consumption, the depletion of hydrocarbon reserves and the global warming drive the need for innovative technologies in energy conversion and storage. Supercapacitors, also known as ultracapacitors or ionistors, have attracted increasing popularity in recent years due to their high-power density, fast charging, long lifetime and safety. However, the widespread use of supercapacitors is restricted by their low capacitance (compared to that of lithium-ion batteries<sup>1</sup>) and electrochemical stability.<sup>2,3</sup> In this regard, the development of new materials and approaches to the production of supercapacitors with high specific capacitance and long-term stability is an important problem of considerable current interest. Graphene, which is characterized by the highest electrical conductivity and specific surface area, is a promising material for supercapacitor electrodes.<sup>4–7</sup> However, the materials based on graphene sheets tend to show a low capacity (100–200 F g<sup>-1</sup>).<sup>8,9</sup> One way to increase the capacitance of graphene materials is the introduction of redox-active fragments.<sup>10</sup>

In this paper, we propose an approach that includes the covalent modification of graphene oxide (GO) by 3,3',4,4'-tetraaminodiphenyl oxide (TADPO)<sup>†</sup> molecules accompanied by the reduction of oxygen-containing groups and the formation of three-dimensional grids (GO-TADPO). For the first time, we used TADPO molecules grafted on the surface of GO. TADPO was chosen as a modifier due to its solubility in water at elevated temperatures and the formation of benzimidazole rings as a result of its interaction with GO. The presence of benzimidazole rings is capable of increasing the capacitance of a supercapacitor due to participation in reversible Faradaic processes.<sup>11</sup>

<sup>†</sup> Graphite oxide was obtained by the oxidation of natural graphite according to a Hummers method.<sup>12</sup> TADPO was purified by recrystallization from water with activated charcoal. The melting point of TADPO was 150–151 °C.

**Table 1** Elemental analysis data for GO, RGO and GO-TADPO (wt%).

Sample	C	H	N	O
GO	50.1	2.2	0	47.7
RGO	74.3	1.8	0	23.9
GO-TADPO	66.4	3.1	13.8	16.7

The GO-TADPO material was obtained *via* a one-step synthesis using an ecologically sound and highly effective hydrothermal method.<sup>‡</sup> In comparison, the reduced graphene oxide (RGO) sample was obtained without the use of TADPO under similar conditions. The resulting materials were characterized by IR spectroscopy and elemental analysis.<sup>§</sup> According to the latter (Table 1), the nitrogen content of the GO-TADPO material was 13.8%. Note that the partial reduction of the GO also occurred to cause a lower oxygen content of the RGO.

<sup>‡</sup> To obtain the GO dispersion, the resulting graphite oxide was sonicated using a Sapiro UZV-2.8 ultrasonic bath (power, 100 W; frequency, 35 kHz) followed by centrifugation at 2000 rpm for 2 h. TADPO (115 mg) was added to the dispersion of GO (50 ml, 1.3 mg ml<sup>-1</sup>) with stirring. The resulting solution was transferred to a Teflon-lined autoclave and heated at 180 °C for 12 h in an argon atmosphere. After cooling the autoclave to room temperature, the mixture was stirred with isopropanol for the complete removal of unreacted TADPO. The product was then filtered through a Teflon membrane filter (pore size, 0.2 μm; Vladisart), washed several times with isopropanol and finally vacuum-dried for 12 h at 50 °C and 6 h at 150 °C.

<sup>§</sup> Elemental analysis was performed using a Vario Micro cube CHNS analyzer (Elementar). The IR spectra were recorded on an Alpha spectrometer (Bruker) in a wavenumber range of 4000–400 cm<sup>-1</sup> using KBr tablets. TGA was carried out on a STA 449 C14/G Jupiter instrument (Netzsch) at a heating rate of 10 K min<sup>-1</sup> in a flow of argon. The X-ray diffraction patterns were recorded using a D8 Advance AXS diffractometer (Bruker) with CuKα radiation.

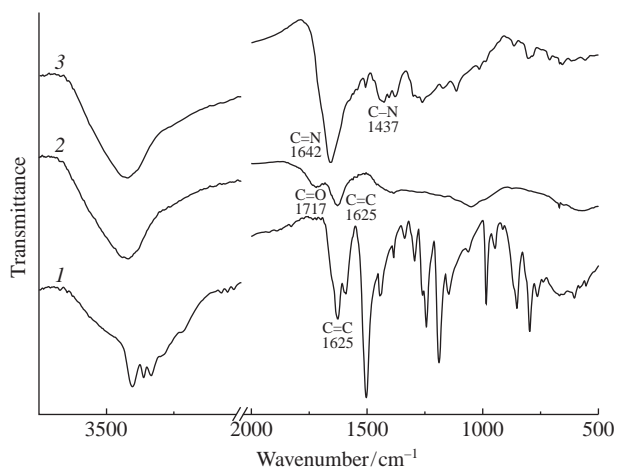


Figure 1 IR spectra of (1) TADPO, (2) GO and (3) GO-TADPO.

IR spectroscopy was used to determine the nature of interaction between GO and TADPO (Figure 1). Characteristic absorption bands due to C=C bonds at  $1625\text{ cm}^{-1}$  and the C=O bonds of carboxylic groups at  $1717\text{ cm}^{-1}$  were observed in the spectrum of GO; however, the peak of C=O bonds disappeared after the modification. In the spectrum of GO-TADPO, new peaks at  $1642$  and  $1437\text{ cm}^{-1}$  were detected; they can be attributed to the C=N and C–N bonds of benzimidazole rings. In addition, there were no absorption bands due to amino groups in the spectrum of GO-TADFO in a range of  $3300\text{--}3500\text{ cm}^{-1}$ , whereas they were present in the spectrum of TADPO.

The resulting material and the initial GO and TADPO were studied by TGA (Figure 2). The intense thermal destruction of GO due to the decomposition of oxygen-containing functional groups commenced at  $200^\circ\text{C}$ . The weight loss at  $500^\circ\text{C}$  exceeded 50%. The temperature of the onset of TADPO destruction was  $280\text{--}300^\circ\text{C}$ , and less than 40% of the initial weight was retained at  $500^\circ\text{C}$ . In contrast to the initial compounds, GO-TADPO showed only a 10% weight loss at  $500^\circ\text{C}$ . The higher thermal stability of the resulting material was due to the partial reduc-

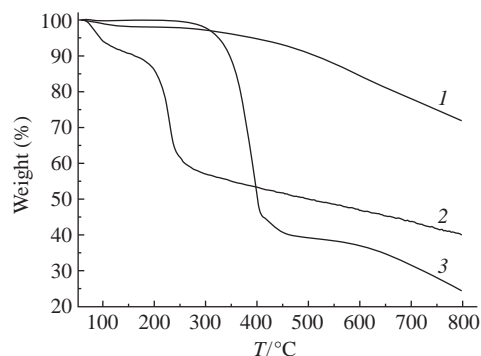
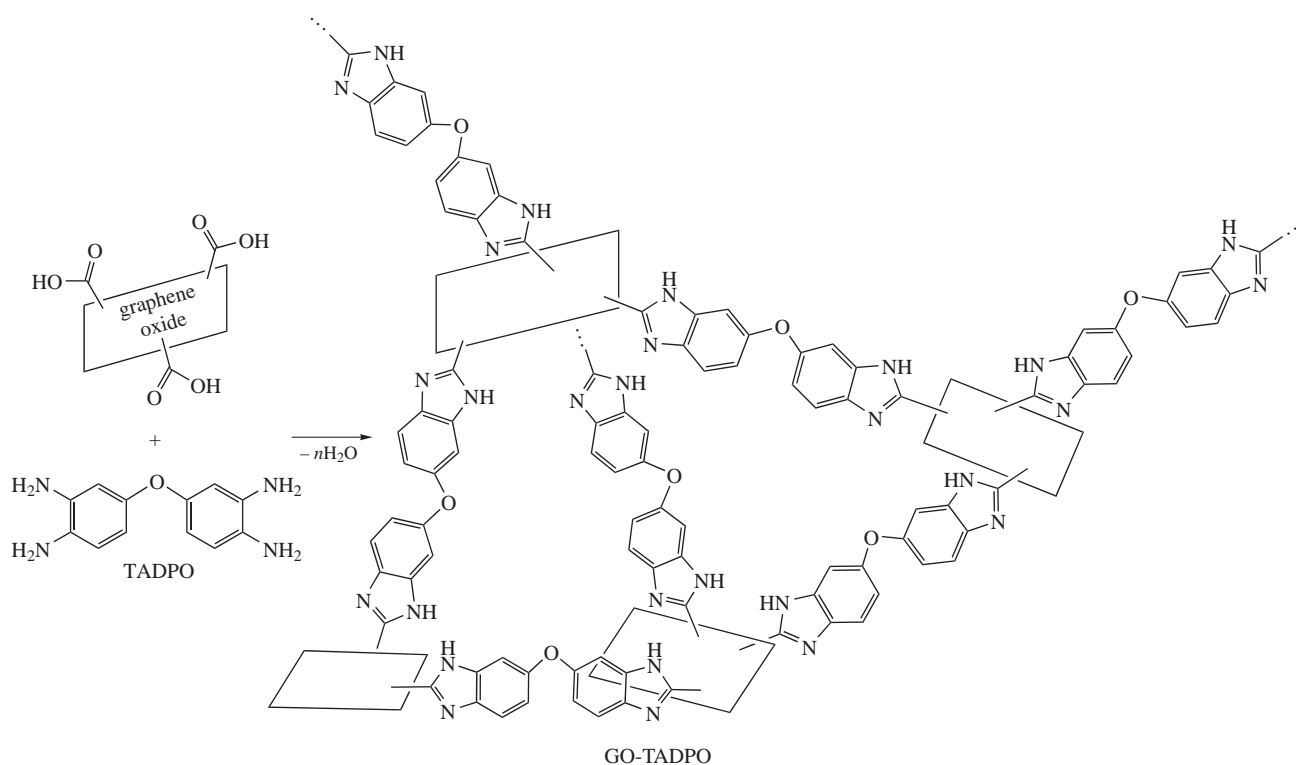


Figure 2 TGA curves of (1) GO-TADPO, (2) GO and (3) TADPO.

tion of oxygen-containing groups during the synthesis and the conversion of carboxyl groups into more heat-resistant benzimidazole rings. These data allow us to infer that, in the course of hydrothermal synthesis, the carboxyl groups of GO and the *o*-diamine groups of TADPO interact to form benzimidazole rings.

The X-ray diffraction patterns of the GO-TADPO contain only a broad halo in a range of  $11\text{--}25^\circ$ , which indicates the formation of an amorphous phase because of the covalent grafting of benzimidazole rings. Moreover, there is no reflex at *ca.*  $12^\circ$  typical of graphite oxide. In addition, the inability of GO-TADPO to disperse in both water and organic solvents (alcohols, amide solvents, methanesulfonic acid, *etc.*) indicates the formation of three-dimensional crosslinked structures (Scheme 1).

To estimate the prospects of the GO-TADPO as a supercapacitor electrode material, we characterized its electrochemical properties by standard cyclic voltammetry (CV). Figure 3 shows that a difference between the CV curves of RGO and GO-TADPO is significant. A substantial contribution to the electrochemical properties of GO-TADPO is made by a reversible redox process in benzimidazole rings, which corresponds to peaks at  $\sim 680\text{ mV}$  in the charge curve and  $\sim 350\text{ mV}$  in the discharge curve.<sup>11</sup> The lower height of an anode peak, as compared with a cathode one, indicates the partial irreversibility of such redox reactions. The



GO-TADPO

Scheme 1

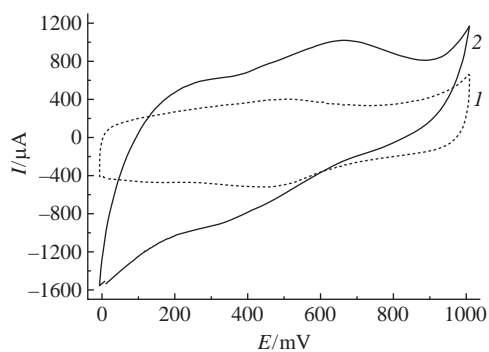


**Figure 3** CV curves of (1) RGO and (2) GO-TADPO at a scan rate of  $2 \text{ mV s}^{-1}$ .

specific capacitance of GO-TADPO was  $330 \text{ F g}^{-1}$  at a scan rate of  $2 \text{ mV s}^{-1}$ , while that of RGO was  $169 \text{ F g}^{-1}$ , which also confirms the major influence of redox processes in benzimidazole rings on the capacitance.<sup>†</sup>

In summary, the interaction between GO and TADPO under hydrothermal synthesis conditions makes it possible to prevent the agglomeration of graphene sheets due to the formation of three-dimensional grids. The material formed has a high capacitance owing to the cross-linked three-dimensional structure and the presence of redox-active benzimidazole rings; thus, it is promising for the development of high-performance supercapacitors.

<sup>†</sup> The electrochemical performance characteristics of materials were studied using an Elins P-30SM potentiostat with a standard three-electrode cell system using a  $3.5 \text{ M}$  aqueous solution of  $\text{H}_2\text{SO}_4$  as an electrolyte. The working electrode was obtained by mixing the test material with carbon black and Vaseline oil in a weight ratio of 80:10:10.<sup>13,14</sup> The resulting mixture was blended thoroughly in an agate mortar and applied to a graphite rod. A platinum plate and a silver chloride electrode were used as auxiliary and reference electrodes, respectively. The potentials were measured relative to a saturated silver–silver chloride reference electrode.

This study was supported by the Russian Foundation for Basic Research (grant no. 16-33-00218 mol\_a).

## References

- 1 T. L. Kulova, Yu. M. Kreshchenova, A. A. Kuz'mina, A. M. Skundin, I. A. Stenina and A. B. Yaroslavl'tsev, *Mendeleev Commun.*, 2016, **26**, 238.
- 2 L. Kouchachvili, W. Ya'ici and E. Entchev, *J. Power Sources*, 2018, **374**, 237.
- 3 L. Zhang, X. Hu, Z. Wang, F. Sun and D. G. Dorrell, *Renew. Sustain. Energy Rev.*, 2018, **81**, 1868.
- 4 J. P. Mensing, C. Poochai, S. Kerdpocha, C. Sriprachubwong, A. Wisitsoraat and A. Tuantranont, *Adv. Nat. Sci.: Nanosci. Nanotechnol.*, 2017, **8**, 033001.
- 5 Y. Liu and X. Peng, *Appl. Mater. Today*, 2017, **8**, 104.
- 6 X. Chen, R. Paul and L. Dai, *Natl. Sci. Rev.*, 2016, **4**, 453.
- 7 A. A. Arbuzov, S. A. Mozhzhukhin, A. A. Volodin, P. V. Fursikov and B. P. Tarasov, *Russ. Chem. Bull., Int. Ed.*, 2016, **65**, 1893 (*Izv. Akad. Nauk, Ser. Khim.*, 2016, 1893).
- 8 T. Y. Kim, H. W. Lee, M. Stoller, D. R. Dreyer, C. W. Bielawski, R. S. Ruoff and K. S. Suh, *ACS Nano*, 2011, **5**, 436.
- 9 M. D. Stoller, S. Park, Y. Zhu, J. An and R. S. Ruoff, *Nano Lett.*, 2008, **8**, 3498.
- 10 M. Yu, B. Xie, Y. Yang, Y. Zhang, Y. Chen, W. Yu, S. Zhang, L. Lu and D. Liu, *RSC Adv.*, 2017, **7**, 15293.
- 11 W. Ai, W. Zhou, Z. Du, Y. Du, H. Zhang, X. Jia, L. Xie, M. Yi, T. Yu and W. Huang, *J. Mater. Chem.*, 2012, **22**, 23439.
- 12 W. S. Hummers, Jr. and R. E. Offeman, *J. Am. Chem. Soc.*, 1958, **80**, 1339.
- 13 N. F. Uvarov, Yu. G. Mateyshina, A. S. Ulihin, S. I. Yusin, V. I. Varentsova and V. K. Varentsov, *ECS Trans.*, 2010, **25**, 11.
- 14 A. A. Shibaev, S. I. Yusin, E. A. Maksimovskii, A. V. Ukhina and A. G. Bannov, *Russ. J. Appl. Chem.*, 2016, **89**, 739 (*Zh. Prikl. Khim.*, 2016, **89**, 605).

Received: 26th July 2017; Com. 17/5319